In Situ STM and Electrochemical Investigation of Sulfur Oxidative Underpotential Deposition on Ag(111)

Giovanni D. Aloisi, Massimiliano Cavallini, Massimo Innocenti, Maria Luisa Foresti, Giovanni Pezzatini, and Rolando Guidelli*

Dipartimento di Chimica, Università di Firenze, Via G.Capponi 9, 50121 Firenze, Italy

Received: November 20, 1996; In Final Form: March 18, 1997[⊗]

The oxidative underpotential deposition of sulfur on Ag(111) from alkaline solutions of Na_2S was investigated by in situ scanning tunneling microscopy (STM), cyclic voltammetry, and chronocoulometry. Proceeding toward more positive potentials, the cyclic voltammetric curve shows three partially overlapping peaks A−C and an isolated and more acute peak D. The STM images of the overlayer of adsorbed sulfur over the potential region between peaks C and D reveal a $(\sqrt{3} \times \sqrt{3})$R30° structure; those at potentials positive to peak D a $(\sqrt{7} \times \sqrt{7})$R19° structure: each lattice site of the latter structure is occupied by a triplet of sulfur atoms. The fractional coverage, $^1/_3$, for the $(\sqrt{3} \times \sqrt{3})$R30° structure is in perfect agreement with the maximum surface concentration, $\Gamma_{max} = 7.7 \times 10^{-10}$ mol cm^{-2}, obtained from a thermodynamic analysis of the chronocoulometric charge vs potential curves; $2F\Gamma_{max}$ is about 10% larger than the charge associated with the combination of peaks A−C. On the other hand, the $2F\Gamma$ value corresponding to the fractional coverage, $^3/_7$, for the $(\sqrt{7} \times \sqrt{7})$R19° structure agrees satisfactorily with the charge associated with the sum of peaks A−D, thus suggesting a total electron transfer from sulfide ions to the metal over the range of stability of the latter structure.

1. Introduction

The interest in monolayer adsorption of sulfur on single-crystal faces of metal electrodes has recently received new impetus by studies on the electrochemical growth of structurally well-defined semiconductor thin films. These materials are promising candidates for the use in light-emitting and photovoltaic devices and in several optoelectronic applications as well. An important advance in the atomic-level control of the electrodeposition processes has been reported by Stickney and co-workers,[1] who have developed an electrochemical analogue of conventional atomic layer epitaxy (ECALE); this procedure has been employed to produce well-ordered deposits of compound semiconductors, such as CdTe and CdS, on gold polycrystalline and single-crystal electrodes. Preliminary electrochemical studies of CdTe electrodeposition on polycrystalline Pt and Cu electrodes were also carried out.[2] The use of silver in place of gold as a support of compound semiconductors seems attractive, in view of its lower cost; moreover, polycrystalline (111)-oriented Ag film electrodes deposited on mica or quartz surfaces can be obtained by Ag evaporation under vacuum, with the same ease as Au films. Hence, from a technological point of view Ag appears to be a promising candidate for device fabrication.

Our interests are in the initial stages of the electrodeposition of thin films of compound semiconductors on Ag single-crystal faces. The present study deals with a scanning tunneling microscopy (STM) structural investigation of sulfur ordered overlayers on Ag(111). Since these overlayers have different structures depending on the applied potential and their formation is accompanied by a current flow, a parallel electrochemical investigation is also described. This study precedes an investigation of the electrodeposition of S on Ag(111) followed by the reductive underpotential deposition (upd) of Cd on the S/Ag-(111) surface: this will be the subject of a future paper.

While the structural features of the oxidative upd of sulfur from aqueous Na_2S have been investigated on Au(111),[3] no similar in situ surface-sensitive structural analysis has been so far reported on Ag(111). On the other hand, the oxidative upd of sulfur has been extensively investigated on polycrystalline Ag by voltammetric and radiolabeling methods[4−6] and, more recently, on the low-index faces of Ag by cyclic voltammetry.[7] In particular, Hatchett and White[7b] hypothesized a $(\sqrt{7} \times \sqrt{7})$-R10.9° structure for sulfur overlayers on Ag(111), on the basis of coulometric measurements of interfacial charge and of electrochemical quartz crystal microbalance (EQCM) measurements of mass. Sulfur overlayers on the low-index faces of silver were examined in uhv by Rovida and Pratesi[8] using LEED-Auger techniques; on Ag(111) these authors reported a "D phase", with a $(\sqrt{7} \times \sqrt{7})$R19.1° structure. More recently, Heinz and Rabe[9] imaged Ag(111) films on mica, previously immersed in diluted aqueous solutions of Na_2S and H_2S, by ex situ STM under atmospheric conditions: a $(\sqrt{7} \times \sqrt{7})$R10.9° structure was reported.

2. Experimental Section

Merck Suprapur NaF was baked at 700 °C to remove organic impurities. Merck Suprapur NaOH and Aldrich analytical reagent grade Na_2S were used without further purification. The water used was obtained from light mineral water by distilling it once and by then distilling the water so obtained from alkaline permanganate while constantly discarding the heads. The solutions were freshly prepared just before the beginning of each series of measurements; in fact, aged sulfide solutions yielded in situ STM images of well-resolved polysulfide chains on Ag-(111) that were not observed when using freshly prepared solutions. The working electrodes were cylindrical silver crystals grown in a graphite crucible, oriented by X-rays, and cut according to the Bridgman technique.[10] These electrodes were polished with successively finer grades of alumina power down to 0.3 μm (Buehler Micropolish II) and then annealed in a muffle furnace under vacuum for 30 min at 650 °C. All potentials are referred to the saturated calomel electrode (SCE).

STM Measurements. The STM employed was a standard TMX 2000 system by Topometrix, modified for in situ

[⊗] Abstract published in *Advance ACS Abstracts,* May 1, 1997.

S1089-5647(96)03873-4 CCC: $14.00

electrochemistry as described in ref 11. Both constant-height and constant-current imaging modes were used, as noted in the legends. The exact tunneling conditions are also given in the legends. A positive bias voltage indicates that the tip was positive relative to the sample. W tips were used; they were prepared from 0.25-mm-diameter W wire (Aldrich) by electrochemical ac etching in 1 M KOH solution. For insulation the etched tips were coated with Apiezon wax. Unless otherwise indicated in the legend, all images presented are unfiltered.

The Ag(111) electrode was a cylinder 4 mm in diameter and 2.4 mm in height. The reference electrode was a homemade saturated AgCl electrode joined to the working solution through a double-junction reservoir containing 0.1 M NaF, to avoid leakage of sulfide ions into the reference electrode and of chloride ions into the electrochemical cell. The auxiliary electrode was a platinum wire 0.5 mm in diameter. The volume of the cell was 150 μL. Before the STM cell was assembled, all components were washed in concentrated sulfuric acid and rinsed repeatedly with water to remove any traces of the acid. After mechanical polishing, the electrode was etched for a few seconds with a 1:1 (v/v) mixture of 40% H_2O_2 and 30% NH_3 to remove the outermost, distorted lattice layers. Moreover, prior to each measurement, the electrode was etched mildly with a mixture of 90% water and 10% of the above etching solution; the electrode was then washed with 10% NH_3 and finally with water. This procedure ensured an oxide-free surface. STM measurements were carried out only after verifying the good quality of the electrode surface by recording a cyclic voltammogram in 10^{-2} M NaF. The presence of oxygen was found not to affect the voltammetric peaks for sulfur upd; hence, STM measurements were constantly carried out without deaerating the solution.

Electrochemical Measurements. Before each electrochemical measurement the electrode was polished chemically with CrO_3 according to the procedure described in ref 12. After polishing, the electrode surface was soaked in concentrated sulfuric acid for about 20 min and then rinsed thoroughly with water. A gold wire was used as a counter electrode, and an external saturated calomel electrode (SCE) served as reference. The four-electrode potentiostatic system by Herrmann et al.[13] was employed to minimize the noise, and positive feedback circuitry was utilized to correct for the uncompensated resistance. The hanging solution method[14] was employed. The cell was water-jacketed and thermostated at 25 ± 0.2 °C. The solution was deaerated with argon that was bubbled into the solution before measurements and flown over the solution during them. The cylindrical single-crystal electrode was held by a silver wire sealed into a glass tube which was secured to a movable stand; the latter was moved up or down at an adjustable rate by means of an oleodynamic piston which ensured the complete absence of vibrations. A pressure gauge connected to the oleodynamic system permitted us to reproduce the optimum rate (1.5 mm/s). The stand was connected to a digital position sensor, which permitted us to estimate a 0.1 mm vertical shift of the stand. The wholly computerized instrumentation for differential capacity and capacitive charge measurements is described elsewhere.[15]

3. Results

Electrochemical Measurements. Voltammetric measurements were carried out in solutions made alkaline with 0.1 M NaOH, because at lower pH values hydrogen evolution masks the most negative peak due to sulfur upd. In view of the two pK_a values of H_2S, ≈7 and ≈15,[16] under the experimental conditions adopted herein only one sulfur-containing species is present in the solution, i.e., HS^-.

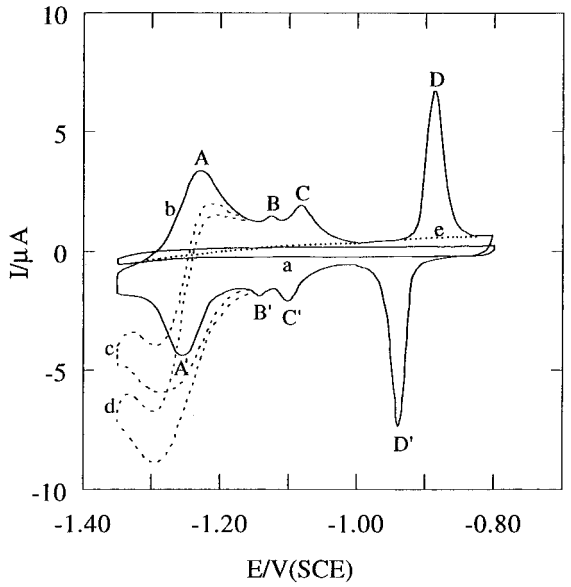

Figure 1. Cyclic voltammetric response of Ag(111) in aqueous 0.1 M NaOH both in the absence (a) and in the presence of 1×10^{-3} M Na_2S (b). The cyclic voltammograms c and d were obtained in the same solution as voltammogram b after continuous cycling between −1.35 and −0.80 V for 15 and 30 min, respectively. The charge involved in the sum of the voltammetric peaks A−C as well as that involved in the single peak D were obtained by measuring the area enclosed between these peaks and the dotted curve e. Electrode area = 0.070 cm^2. Scan rate = 50 mV s^{-1}.

Figure 1 shows the ciclic voltammogram of 0.1 M NaOH on Ag(111), both in the absence (curve a) and in the presence of 1×10^{-3} M Na_2S (curve b). While the voltammogram of 0.1 M NaOH alone is featureless, that in the presence of sulfide exhibits four anodic peaks A−D, with peak potentials equal to −1.23, −1.13, −1.08, and −0.89 V/SCE. The cathodic peaks A′, B′, and C′ are shifted in the negative direction by only ≈20 mV with respect to their anodic counterparts, whereas peak D′ is more negative by 60 mV with respect to peak D. Peak B is small, and in some cases it is not detected. At potentials positive to −0.75 V bulk sulfur deposition takes place. These positive potentials were therefore carefully avoided, because this deposition tends to spoil the electrode surface by roughening it. The voltammogram in Figure 1 is similar to that obtained by Hatchett et al. under almost identical conditions [Figure 3 in ref 7a]. Our measurements differ from Hatchett's mainly by (i) the presence of peak B, (ii) an appreciable hydrogen discharge at far negative potentials when in the presence of sulfide, (iii) a cyclic voltammogram of 0.1 M NaOH alone that merges with that in the presence of sulfide neither between peaks C and D nor at potentials positive to peak D. The occasional appearance of the small peak C in our cyclic voltammograms seems to be related to the surface state, in that it is usually observed with freshly cut Ag(111) electrodes, with extended atomically flat terraces.

Hydrogen evolution at the more negative potentials increases dramatically with repeated potential cycling, such that after $^1/_2$ h of continuous cycling it gives rise to a notable cathodic current that distorts peak A and ultimately obliterates it. This is clearly apparent from curves c and d in Figure 1, obtained after subjecting the electrode to continuous cycling between −1.35 and −0.80 V for 15 and 30 min, respectively. The cathodic current due hydrogen evolution shows an unusual behavior, in that it decreases when scanning the potential from ≈−1.30 to −1.35 V, giving rise to a cathodic peak. That this peak is not due to the reduction of some species that is consumed on the electrode surface is indicated by the positive-going run, which

is roughly parallel to the preceding negative-going one. Moreover, by stepping the applied potential from any value positive to the hydrogen evolution "peak" to any value along the peak, the resulting current is constant in time: this indicates that the current is fed by a species that is not consumed on the electrode, namely, by water itself. As will be shown in describing STM results, the increasing hydrogen evolution with continuous cycling is to be ascribed to a progressive accumulation of sulfur atoms adsorbed at surface defects on the Ag(111) face; these sulfur atoms are not completely removed by reduction to HS^- even at -1.35 V, although the potential scan from -1.30 to -1.35 V causes a temporary decrease in their amount, and hence in the extent of hydrogen evolution. At still more negative potentials hydrogen evolution takes place even in the absence of sulfide ions, and the reduction current due to hydrogen evolution increases again. A catalytic effect by sulfur atoms adsorbed at Ag(111) upon hydrogen evolution was also reported by Protopopoff and Marcus.[17]

The initial situation exemplified by the cyclic voltammogram of Figure 1, curve b, and characterized by a modest hydrogen evolution at -1.35 V, is readily restored by chemical polishing with CrO_3. Nonetheless, even this modest hydrogen evolution decreases the accuracy with which the charge associated with the combination of peaks A−C can be measured. Moreover, the voltammetric curve of 0.1 M NaOH alone (curve a in Figure 1) does not merge with that in the presence of Na_2S after peak D, thus preventing a completely unambiguous subtraction of the double-layer charging current. At any rate, the charge computed by measuring the area enclosed between the voltammetric peaks A−C and the dotted curve e in Figure 1 amounts to 130 ± 3 μC cm^{-2}, whereas that enclosed between peak D and the dotted curve e equals 55 ± 3 μC cm^{-2}. These two values should be compared with those, 114 and 92 μC cm^{-2}, determined by Hatchett et al.[7] for the same system. The coulometric charge associated with the steady-state voltammetric peaks at a scan rate of 50 mV/s is independent of the Na_2S concentration, c, for $c > 5 \times 10^{-4}$ M. An increase in c causes a gradual shift of these peaks toward more negative potentials.[7a]

The charge involved in the stepwise upd of sulfur was estimated more accurately by using potential-step chronocoulometry. To this end the applied potential was stepped from a variable initial value E to a fixed final value $E_f = -1.35$ V, at which sulfide desorption is rapid and almost complete, and the current following the potential step $E \rightarrow E_f$ was integrated over time. The initial potential E was progressively varied from -1.45 to -0.80 V by 25 mV increments. The rest time of the electrode at E was made long enough to ensure the attainment of adsorption equilibrium. The plots of the charge density $Q(E,t)$ vs time t so obtained show an abrupt rise followed by a modest linear increase in time, due to the constant current for hydrogen evolution at E_f. Linear extrapolation of these plots to $t = 0$ yields the charge density, Q_0, corrected for the faradaic contribution due to hydrogen evolution. Curve b in Figure 2 shows a plot of Q_0 vs E. Proceeding toward positive potentials, this plot shows a slight inflection corresponding to the transition from peak A to peaks (B + C), and two well-defined plateaus corresponding to the potential region between peaks C and D and to the region positive to peak D, respectively. Curve a in Figure 2 is the Q_0 vs E plot provided by aqueous 0.1 M NaOH under otherwise identical conditions. The vertical distance between the first plateau of curve b and curve a is a measure of the charge involved in sulfur upd along the voltammetric peaks A−C; it amounts to 125 ± 3 μC cm^{-2} and is therefore only slightly less than the value, 130 ± 3 μC cm^{-2}, obtained from the area under the corresponding voltammetric peaks. The

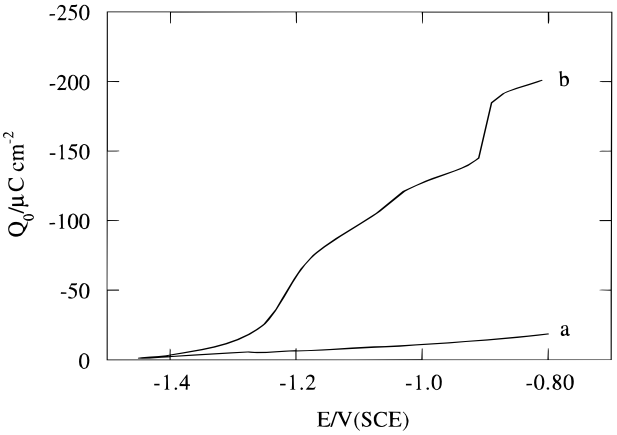

Figure 2. Chronocoulometric charge vs potential curve for Ag(111) in aqueous 0.1 M NaOH both in the absence (a) and in the presence of 1×10^{-3} M Na_2S (b).

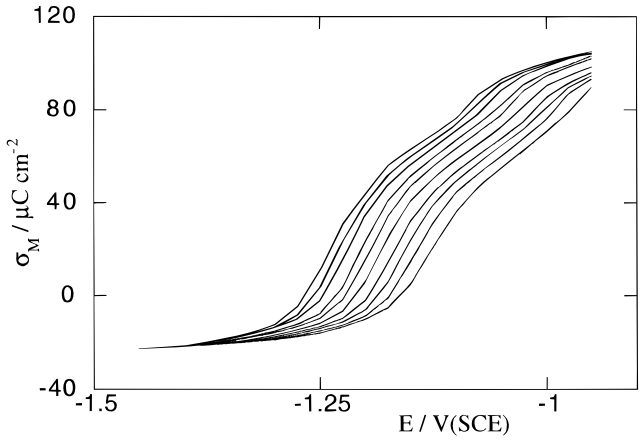

Figure 3. Plots of σ_M vs E for sulfide adsorption on Ag(111) from solutions of 0.1 M NaOH + cM Na_2S. Proceeding upward, c equals 2×10^{-6}, 5×10^{-6}, 1×10^{-5}, 2×10^{-5}, 5×10^{-5}, 1.17×10^{-4}, 2.2×10^{-4}, 5.95×10^{-4}, 1.07×10^{-3}, 1.92×10^{-3}, and 4.5×10^{-3} M.

chronocoulometric value must be regarded as more accurate, since it is corrected satisfactorily for the charge due to the hydrogen evolution reaction. The vertical distance between the second plateau and curve a measures the whole charge due to sulfur upd and amounts to 185 ± 3 μC cm^{-2}. The difference, $185 - 125 = 60$ μC cm^{-2}, between the two chronocoulometric charge values is in good agreement with the charge, 55 μC cm^{-2}, estimated from the area under peak D. Conversely, it is appreciably less than the value, 92 μC cm^{-2}, reported by Hatchett et al.[7]

A thermodynamic analysis of sulfide adsorption on Ag(111) was carried out at potentials negative to peak D on the basis of experimental curves of the capacitive charge density σ_M vs E, as recorded by the chronocoulometric technique. Figure 3 shows a series of σ_M vs E curves obtained from solutions of 0.1 M NaOH + c M Na_2S, with c ranging from 2×10^{-6} to 4.5×10^{-3} M. The detailed procedure adopted to obtain these curves is described in ref 18. Briefly, $Q_0(E)$ vs E curves exactly analogous to that in Figure 3 were first obtained for the various sulfide concentrations; these curves were converted into σ_M vs E curves by forcing them to coincide at -1.45 V, where sulfide desorption is complete, and by then setting the common σ_M value at -1.45 V equal to that for aqueous 0.1 M NaF. At the lowest sulfide concentration investigated the rest time at E required to attain adsorption equilibrium was found to be 20 min. No attempt was made to cover the potential region of peak D, because of the irreproducibility in the rising section

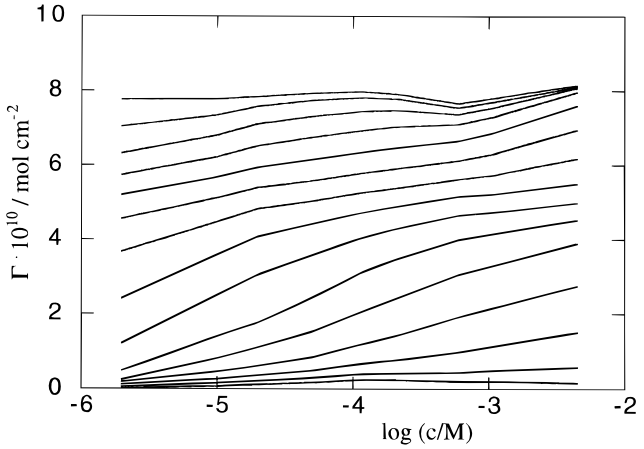

Figure 4. Plots of Γ vs log c for sulfide adsorption on Ag(111) from aqueous 0.1 M NaOH at different applied potentials. Proceeding upward, E increases from −1.300 to −0.950 V by 25 mV increments.

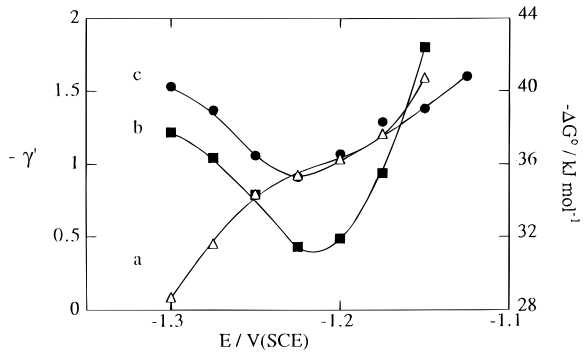

Figure 5. Plots of $-\Delta G^\circ$ vs E (a), $-\gamma' = -(\partial \Delta G^\circ/\partial E)_\Gamma/F$ vs E (b), and $-\gamma' = (\partial \sigma_M/\partial \Gamma)_E/F$ vs E (c) for sulfide adsorption on Ag(111) from aqueous 0.1 M NaOH.

(but not in the height) of the $Q_0(E)$ vs E step corresponding to this voltammetric peak.

To a very good approximation, the electrocapillary equation in the presence of the strong excess of NaOH takes the simplified form[19]

$$-\mathrm{d}\gamma = \sigma_M \,\mathrm{d}E + \Gamma RT \ln c$$

where γ is the interfacial tension and Γ is the surface excess of the sulfide ions. To calculate Γ, the σ_M vs E curves in Figure 3 were integrated to give relative γ vs E plots. Next, the relative interfacial tension at constant E was plotted vs ln c and the resulting curves were differentiated to yield Γ. Figure 4 shows plots of Γ vs log c at different applied potentials E. These plots exhibit the typical sigmoidal shape only at potentials negative to −1.150 V. With a further positive shift in E the surface excess at the lowest concentration investigated increases, until it attains a concentration-independent maximum value $\Gamma_{max} = 7.7 \times 10^{-10}$ mol cm^{-2}. This value corresponds to a charge density σ_i of the specifically adsorbed sulfide ions equal to $2F\Gamma_{max} = 148\ \mu$C cm^{-2}. The standard Gibbs energy of adsorption, ΔG°, was determined as a function of E by extrapolating plots of $\ln(-\sigma_i/c)$ vs σ_i at constant E to $\sigma_i = 0$. According to the virial isotherm,[20] commonly employed for ionic electrosorption, the intercept of this plot on the vertical axis equals $-\Delta G^\circ/(RT)$. Values of $-\Delta G^\circ$ as obtained by this extrapolation procedure are plotted against E in Figure 5, curve a; these values refer to a standard state of unit molarity in solution and 1 ion cm^{-2} on the metal surface. The derivative of ΔG° with respect to E is equal to the electrosorption valency γ'.[21,22] This quantity can also be determined independently from the derivative of σ_M with respect to Γ at constant E:[23,24]

$$\gamma' = \frac{1}{F}\left(\frac{\partial \Delta G^\circ}{\partial E}\right)_\Gamma = -\frac{1}{F}\left(\frac{\partial \sigma_M}{\partial \Gamma}\right)_E$$

Thus, the slope of σ_M vs Γ plots at low Γ values can be compared with the derivative of ΔG° with respect to E as a further test of the reliability of the ΔG° values. Curves b and c in Figure 5 are plots of the electrosorption valency against potential as obtained by the two alternative procedures. Despite some differences between the two plots, they have a similar shape, indicating that no major errors were made in the data processing. The strongly potential dependent curve of γ' vs E shows some similarities with those reported for the adsorption of chloride[23] and bromide[24] on Au(111), in that it shows a minimum; however, the subsequent maximum exhibited by the latter curves is not observed, although we cannot exclude its presence at the more positive potentials which we were unable to cover due to the scarse reproducibility of charge measurements there.

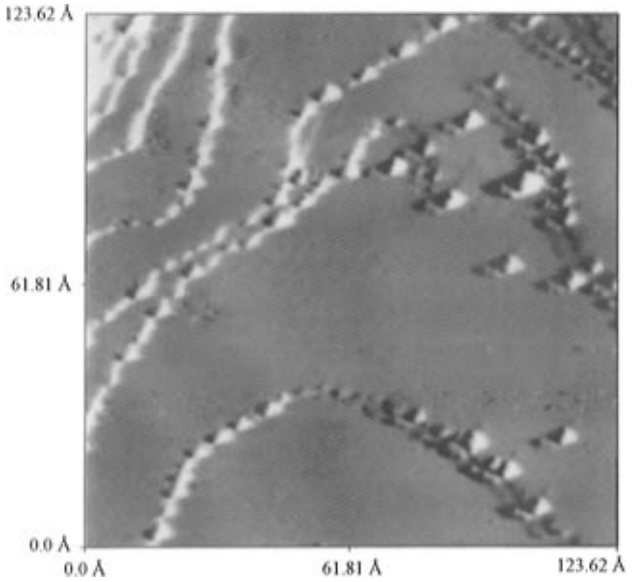

Figure 6. STM image of Ag(111) in aqueous 0.1 N NaOH + 5 × 10^{-4} M Na_2S. Electrode potential $E = -1.3$ V/SCE. Tunneling conditions: bias voltage = 0.8 V, tunneling current = 1.5 nA; constant height mode.

STM Measurements. The nanometer-scale surface morphology and atomic level structure of the Ag(111)/S surface have been investigated by in situ STM. Both in the absence and in the presence of Na_2S, the Ag(111) surface appears to be composed of atomically flat terraces separated by atomic steps. Evidence for this is provided by measuring the step height between adjacent atomically smooth terraces on the Ag(111) and Ag(111)/S surfaces. Images obtained in sulfide solutions at a potential of −1.30 V, where sulfide ions appear to be almost completely desorbed from cyclic voltammetric measurements, reveal the presence of small clusters located along the steps separating adjacent terraces (see Figure 6). These clusters, from 15 to 70 Å wide and about 2 Å high, consist most likely of sulfur atoms and are responsible for the detectable hydrogen evolution observed in cyclic voltammograms at these potentials. The residual presence of sulfur atoms on surface defects at these far negative potentials is not surprising, when we consider that SH^- ions are still adsorbed to an appreciable extent at −1.35 V on stepped surfaces such as Ag(110).[7b]

From −1.3 V to the potential of peak C no images of sulfur atoms are observed on terraces, except for isolated and rather

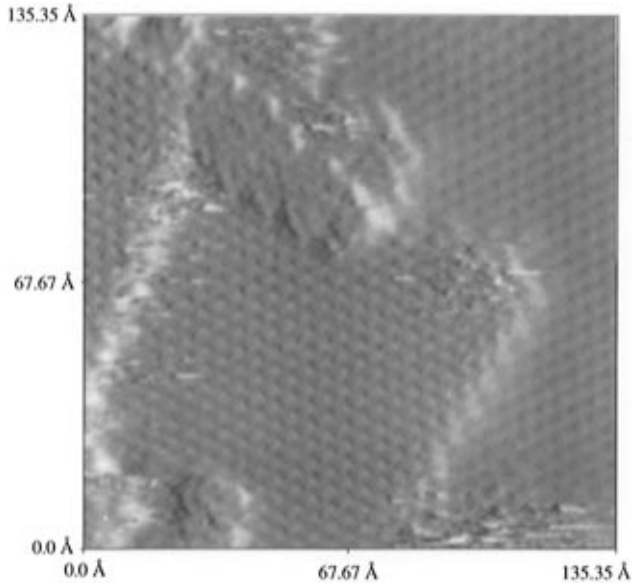

Figure 7. STM image of Ag(111) in aqueous 0.1 N NaOH + 0.7 × 10^{-4} M Na_2S. Electrode potential $E = -0.93$ V/SCE. Tunneling conditions: bias voltage = 0.3 V, tunneling current = 1.5 nA; constant height mode.

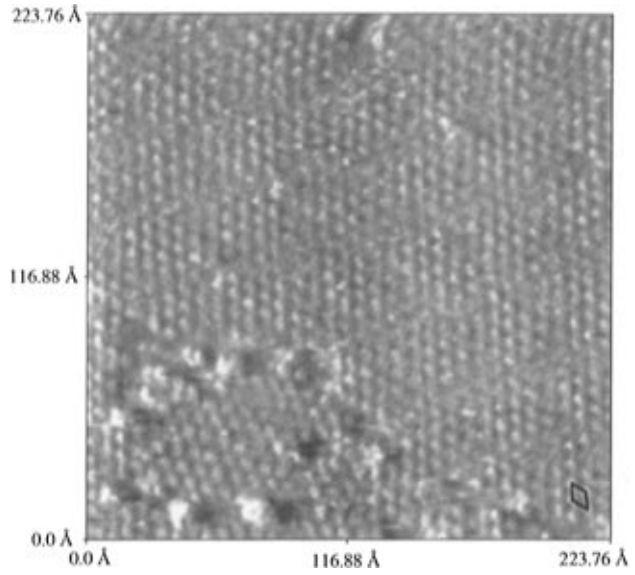

Figure 8. STM image of Ag(111) in aqueous 0.1 N NaOH + 2 × 10^{-4} M Na_2S. Electrode potential $E = -0.71$ V/SCE. Tunneling conditions: bias voltage = 0.25 V, tunneling current = 1.5 nA; constant height mode.

mobile sulfur clusters. At potentials positive to −1.1 V a well-formed structure is observed (see Figure 7), which covers the surface uniformly. This structure can readily be deduced to have the symmetry $(\sqrt{3} \times \sqrt{3})$R30° with respect to the silver substrate lattice. Thus, the spacing between the spots, 5.0 Å, matches well that expected for a $(\sqrt{3} \times \sqrt{3})$ overlayer on silver (i.e., $\sqrt{3} \times 2.88$ Å). Moreover, in STM images containing adjoining patches of substrate lattice and of sulfur overlayer, the rows of bright spots in the overlayer lie in directions midway between (i.e., 30° rotated from) those for the silver substrate. This structure, therefore, consists of adsorbed sulfur atoms with fractional coverage $^1/_3$.

The $(\sqrt{3} \times \sqrt{3})$R30° structure is stable over the potential range from peak C to peak D, which marks the transition to a new hexagonal structure shown in Figure 8. The STM image in this figure shows two domain orientations of the adsorbate, the demain on the lower left region being out of registry with

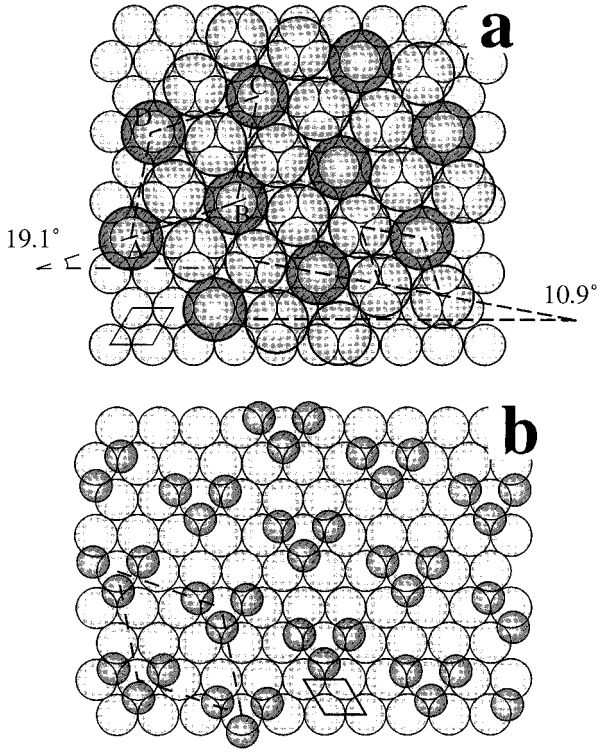

Figure 9. Schematic illustration of two $(\sqrt{7} \times \sqrt{7})$R19° overlayer structures. (a) Rhomb ABCD is the unit cell, smaller circles are silver atoms, larger circles are sulfur atoms, and darker circles form the coincidence lattice. (b) Larger circles are silver atoms; the triplets are arbitrarily centered on the top sites of the substrate lattice.

respect to the larger domain extending throughout the image. The presence of different domains, made evident by the strain at the boundaries, is indicative of adsorption at inequivalent binding sites on the substrate; it also suggests a phase transition occurring via nucleation and growth of different nuclei.[5] The spacing between the bright spots in Figure 8, 8.0 ± 0.1 Å, matches well that expected for a $(\sqrt{7} \times \sqrt{7})$ structure. Moreover, the rows of the overlayer are rotated by 19.1° with respect to those of the silver substrate. This $(\sqrt{7} \times \sqrt{7})$R19.1° structure shows a cross hatch that may be an indication of some modulation, a Moiré pattern, possibly due to compression. This hexagonal structure is just a lattice of atoms adsorbed at equal binding sites: no one-to-one correspondence between lattice sites and sulfur atoms can, however, be postulated, since this would involve a decrease in fractional coverage from $^1/_3$ to $^1/_7$ along peak D, whereas the corresponding flow of charge points unequivocally to an increase in coverage. A familiar structural model that complies with this structure is characterized by a unit cell with two atoms inside and four at the four vertexes (see Figure 9a); along any given row the atoms are adsorbed over a succession of two 3-fold hollow sites and one top site. This model yields a $^3/_7$ fractional coverage. In this case the bright spots in Figure 8 would correspond to the sulfur atoms on top sites. A higher resolution as achieved by increasing the tunneling current (and hence by reducing the distance of the tip from the sample) disproves this hypothesis. In fact, the resulting image of Figure 10 shows that each bright spot in Figure 8 actually consists of a triplet of sulfur atoms. The centers of the sulfur atoms within a triplet form a triangle with two sides of length 2.60 ± 0.05 Å and one of length 3.82 ± 0.08 Å. The spacing between these three atoms should be compared with that, 4.20 ± 0.08 Å, between nearest-neighboring sulfur atoms belonging to adjacent triplets. The short spacing between the atoms of the triplet and the particularly bright area between them strongly suggest some chemical interaction. This

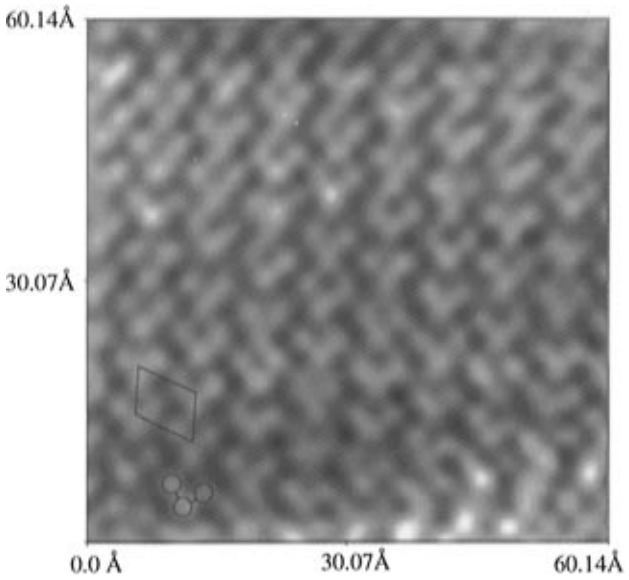

Figure 10. STM image of Ag(111) in aqueous 0.1 N NaOH + 6 × 10^{-4} M Na_2S. Electrode potential $E = -0.82$ V/SCE. Tunneling conditions: bias voltage = 0.075 V, tunneling current = 3 nA; constant current mode. Image filtered by a two-dimensional Fourier transform.

overlayer structure also yields a $^3/_7$ fractional coverage, since each site of the ($\sqrt{7} \times \sqrt{7}$)R19.1° lattice is occupied by a triplet, as shown schematically in Figure 9b.

4. Discussion

The STM images in Figures 7, 8, and 10 permit us to associate peak C with the formation of a $\sqrt{3}$ phase, and peak D with that of a $\sqrt{7}$ phase. Conversely, the absence of atomically resolved images along peak A suggests random chemisorption of relatively mobile sulfur atoms over the corresponding potential range. The origin of peak B, which is observed only occasionally, is dubious; it might be tentatively ascribed to a structure of low fractional coverage, weakly bound to the surface so as to escape STM imaging. The ($\sqrt{3} \times \sqrt{3}$)R30°structure has been deduced commonly for sulfur overlayers on the (111) face of several face-centered cubic transition metals, such as Cu,[25] Pt,[26] Pd,[27] Ir,[28] and Rh,[29] in uhv by low-energy electron diffraction (LEED); it has also been observed by STM with sulfur overlayers on Au(111)[3] and Ag(111)[9] and with alkanethiol films anchored to the surface via the sulfur atom on Au(111)[30] and Ag(111).[9] The ($\sqrt{7} \times \sqrt{7}$)R19.1° structure has also been reported frequently on the (111) face in uhv. Thus, it was first proposed in 1968[25] and confirmed later[31,32] on Cu(111) and clearly observed by STM[33] and LEED[34] on Pd(111). Normally, however, the detailed structural model proposed for the $\sqrt{7}$ phase is that in Figure 9a. This is also true for the sulfur overlayers on Ag(111), where the structural model of Figure 9a was proposed by Schwaha et al.[35] and by Rovida and Pratesi[8] in uhv by LEED and by Heinz and Rabe[9] by STM in ambient conditions; the same model was also proposed for alkanethiolate adlayers on Ag(111).[9,36] It should be noted that all authors investigating sulfur adsorption on Ag(111), with the exception of Rovida and Pratesi,[8] have referred to the structure in Figure 6a as to a ($\sqrt{7} \times \sqrt{7}$)R10.9° structure. As a matter of fact, 10.9° is the lower angle formed by a row of the silver substrate with a vector joining two nearest-neighboring atoms of the sulfur overlayer (see Figure 9a), which occupy two inequivalent binding sites on the substrate. This notation is therefore somewhat misleading, because it is the lower angle formed by one of the vectors of the ($\sqrt{7} \times \sqrt{7}$) unit cell with a row of the substrate, i.e., 19.1°, that expresses the rotation of the overlayer relative to the substrate. A similar pattern of triplets arranged in a ($\sqrt{7} \times \sqrt{7}$)R19.1° structure was proposed for a sulfur overlayer on Pd(111) on the basis of STM measurements in uhv.[33] The structure in Figure 9b can be justified tentatively by the high stability of sulfur trimers,[37] possibly enhanced by the underlying silver atoms. A pattern of selenium trimers arranged in a ($2\sqrt{3} \times 2\sqrt{3}$)R30°−Se unit cell has been recently reported on Au(111) by Lister and Stickney[38] on the basis of in situ STM measurements.

Over the potential range of stability of the $\sqrt{3}$ phase the fractional coverage is $^1/_3$, which corresponds to a surface concentration of sulfide ions equal to $[3(\sqrt{3}/2)(2.88)^2]^{-1}$ ions/Å^2 = 7.7×10^{-10} mol cm^2. This surface concentration practically coincides with the maximum surface concentration Γ_{max} obtained from the thermodynamic analysis over the same potential range (see Figure 4), thus confirming the agreement between thermodynamic and structural data. If such an agreement is to be expected, an agreement between the charges estimated for the $\sqrt{3}$ and $\sqrt{7}$ structures and the actual charges involved in the formation of these structures cannot be taken for granted. Assuming that the number n of electrons released by one sulfide ion following its oxidative upd equals 2, the charge calculated for the $^1/_3$ fractional coverage of the $\sqrt{3}$ phase equals 148 μC cm^{-2}, whereas that for the $^3/_7$ fractional coverage of the $\sqrt{7}$ phase equals 189 μC cm^{-2}. The experimental charge for the $\sqrt{3}$ phase as obtained by integrating the three voltammetric peaks A−C amounts to 130 ± 3 μC cm^{-2}, whereas that for the $\sqrt{7}$ phase as obtained by integrating all four peaks equals 185 ± 3 μC cm^{-2}; the more accurate charge values obtained by chronocoulometry upon correcting for hydrogen evolution, i.e., 125 ± 3 and 185 ± 3 μC cm^{-2}, agree satisfactorily with those obtained from the voltammetric peaks. A comparison of the charge values calculated from the structural data with those measured directly by any of the two electrochemical techniques shows that agreement is quite good for the $\sqrt{7}$ phase, while the calculated value for the $\sqrt{3}$ phase is about 10% larger than the directly measured one. This result can be tentatively explained by assuming that electron transfer from the adsorbed sulfide ions to the electrode is not complete along peaks A−C, while it becomes practically complete along the more positive peak D. At any rate, it should be noted that the experimental charge values are obtained by subtracting from the charge passed in the presence of sulfide ions over a well-defined potential region where sulfide ions undergo upd, the charge passed over the same potential region in the absence of these ions. In this respect, the coincidence of experimental and calculated charge values implies the fulfillment of two requirements: first, that the electron transfer from sulfide ions to the metal upon upd is total; second, that the surface dipole potential due to the electron spillover and to the interfacial solvent molecules is the same at the two ends of the selected potential region both in the absence and in the presence of sulfide ions. While at the end of the potential region at which sulfide ions are still nonadsorbed the second requirement is certainly fulfilled, this is not necessarily the case at the other end. Hence, an exact coincidence between estimated and experimental charge values cannot be taken for granted even if electron transfer is total.

That the surface dipole potential due to the electron spillover and to the solvent molecules plays a role is indicated by the behavior of the electrosorption valency γ' in Figure 5. This quantity coincides with the charge z borne by the adsorbed species under study only if the electron transfer from this species to the electrode is total, and the changes in the surface dipole potential following adsorption are negligible.[21,22] γ' starts to decrease toward more positive potentials in connection with the

voltammetric peak A, tending to the value $z = -2$ as we approach the range of stability of the $\sqrt{3}$ phase. This suggests a gradual electron transfer when proceeding from peak A to peak C. However, γ' also decreases toward more negative potentials, starting from about -1.22 V. The latter behavior is probably to be ascribed to a progressive increase in the orientation of the adsorbed water dipoles with the positive end toward the metal. The displacement of these adsorbed water dipoles from the electrode surface by the adsorbing sulfide ions causes a decrease in their positive contribution to the surface dipole potential, as measured from the metal to the solution. At a constant applied potential E, this decrease must be compensated for by a concomitant increase in the charge density σ_M on the metal surface, and hence in $(\partial\sigma_M/\partial\Gamma)_E = -F\gamma'$, which is greater the more strongly the water dipoles are oriented with their positive end toward the metal. Naturally, the latter effect can only be appreciated when it starts to prevail over the effect of the partial electron transfer from the sulfide ions, which acts in the opposite direction with respect to the applied potential.

A cyclic voltammetric investigation of sulfur overlayers on Ag(111) was recently carried out by Hatchett et al.[7a] in aqueous 0.2 M NaOH, and hence under experimental conditions very close to ours. Even though these authors report cyclic voltammograms very similar to that in Figure 1, the coulometric charge associated with their peaks A + B (corresponding to our peaks A + B + C) equals $\approx$114 μC cm^{-2}, whereas that associated with their peak C (corresponding to our peak D) amounts to $\approx$92 μC cm^{-2}. Retaining our notations for the peaks, the difference between our results and those by Hatchett at al.[7a] is particularly significant for the charge associated with peak D, which we found to amount to 55$-$60 μC cm^{-2} from both cyclic voltammetric and chronocoulometric measurements. In view of the closeness of both their charge values 114 and 92 μC cm^{-2} with the charge, 111 μC cm^{-2}, expected for a fractional coverage of $^1/_2$ with exchange of one electron per sulfur atom, Hatchett et al.[7a] postulate the formation of a compact AgSH adlayer just before peak D: the latter peak should then result from the release of a proton and of a further electron per AgSH adsorbate, with formation of an Ag_2S adlayer. These authors support their conclusions by electrochemical quartz-crystal microbalance (EQCM) measurements, which point to a practical lack of mass change along peak D. In view of our direct charge and structural STM measurements, the charge involved in the formation of peak D corresponds to a fractional coverage of only $^3/_7 - {}^1/_3 = {}^2/_{21}$; hence, if the sensitivity of the EQCM measurements by Hatchett et al.[7a] is of the order of $^1/_{10}$ of a monolayer, the resulting mass change might well have escaped them.

In concluding, we observe that the upd of sulfur from HS^- ions on Ag(111) has several features in common with bromide electrosorption on the same single-crystal face. Thus, when proceeding toward more positive potentials, the cyclic voltammogram of KBr on Ag(111) shows a broad peak, followed by a small hump partially overlapping with it and marking a disorder$-$order transition:[39] this leads to a $(\sqrt{3} \times \sqrt{3})$R30° overlayer of bromide ions, as revealed by in situ STM.[40] A further sharp peak at still more positive potentials marks the transition to a more compressed $(\sqrt{7} \times \sqrt{7})$R19.1° overlayer structure,[40] which differs from the analogous sulfur overlayer structure for being of the type in Figure 9a.

Acknowledgment. The financial support of the Ministero della Ricerca Scientifica e Tecnologica (MURST) and of the Consiglio Nazionale delle Ricerche (CNR) is gratefully acknowledged.

References and Notes

(1) (a) Gregory, B. W.; Stickney, J. L. *J. Electroanal. Chem.* **1991**, *300*, 543. (b) Rhee, C. K.; Huang, B. M.; Wilmer, E. M.; Thomas, S.; Stickney, J. L. *Mater. Manu. Processes* **1995**, *10*, 283.

(2) Gregory, B. W.; Norton, M. L.; Stickney, J. L. *J. Electroanal. Chem.* **1990**, *293*, 85.

(3) Gao, X.; Zhang, Y.; Weaver, M. J. *J. Phys. Chem.* **1992**, *96*, 4156.

(4) Horanyi, G.; Vertes, G. *Electrochim. Acta* **1986**, *31*, 1663.

(5) (a) Birss, V. I.; Wright, G. A. *Electrochim. Acta* **1981**, *26*, 1809. (b) Birss, V. I.; Wright, G. A. *Electrochim. Acta* **1982**, *27*, 1.

(6) Huong, C. N. V.; Parsons, R.; Marcus, P.; Montes, S.; Oudar, J. *J. Electroanal. Chem.* **1981**, *119*, 137.

(7) (a) Hatchett, D. W.; Gao, X.; Catron, S. W.; White, H. S. *J. Phys. Chem.* **1996**, *100*, 331. (b) Hatchett, D. W.; White H. S. *J. Phys. Chem.* **1996**, *100*, 9854.

(8) Rovida, G.; Pratesi, F. *Surf. Sci.* **1981**, *104*, 609.

(9) Heinz, R.; Rabe, J. P. *Langmuir* **1995**, *11*, 506.

(10) Hamelin, A. In *Modern Aspects of Electrochemistry*; Conway, B. E., White, R. E., Bockris, J. O'M., Eds.; Plenum Press: New York, 1985; Vol. 16, p 1.

(11) Aloisi, G. D.; Funtikov, A. M.; Guidelli, R. *Surf. Sci.* **1993**, *296*, 291.

(12) Hamelin, A.; Stoicoviciu, L.; Doubova, L.; Trasatti, S. *J. Electroanal. Chem.* **1988**, *244*, 133.

(13) Herrmann, C. C.; Perrault, G. G.; Konrad, D.; Pilla, A. A. *Bull. Soc. Chim. Fr.* **1972**, *12*, 4468.

(14) Dickertmann, D.; Schultze, J. W.; Koppitz, F. D. *Electrochim. Acta* **1976**, *21*, 967.

(15) Hamelin, A.; Foresti, M. L.; Guidelli, R. *J. Electroanal. Chem.* **1993**, *346*, 251.

(16) Sillén L. G; Martell A. E. *Stability Constants of Metal-Ion Complexes*; The Chemical Society: London, 1964; pp 215$-$216.

(17) Protopopoff, E.; Marcus, P. *J. Chim. Phys.* **1991**, *88*, 1423.

(18) Foresti, M. L.; Innocenti, M.; Hamelin, A. *Langmuir* **1995**, *11*, 498.

(19) Shi, Z.; Lipkowski, J; Gamboa, M; Zelenay, P.; Wieckowski, A. *J. Electroanal. Chem.* **1994**, *366*, 317.

(20) D'Alkaine, C. V.; Gonzalez, E. R.; Parsons, R. *J. Electroanal. Chem.* **1971**, *32*, 57.

(21) Vetter, K. J.; Schultze, J. W. *Ber. Bunsen-Ges. Phys. Chem.* **1972**, *76*, 920, 927.

(22) Schultze, J. W.; Vetter, K. J. *J. Electroanal. Chem.* **1973**, *44*, 63.

(23) Shi, Z.; Lipkowski, J. *J. Electroanal. Chem.* **1996**, *403*, 225.

(24) Shi, Z.; Lipkowski, J.; Mirwald S.; Pettinger B. *J. Chem. Soc., Faraday Trans.* **1996**, *92*, 3737.

(25) Domange, J. L.; Oudar, J. *Surf. Sci.* **1968**, *11*, 124.

(26) (a) Stickney, L. L.; Rosasco, S. D.; Salaita, G. N.; Hubbard, A. T. *Langmuir* **1985**, *1*, 66. (b) Hayek, K.; Glassl, H.; Gutmann, A.; Leonhard, H.; Prutton, M.; Tear, S. P.; Welton-Cook, M. R. *Surf. Sci.* **1985**, *152*, 419. (c) Koestner, R. J.; Salmeron, M.; Kollin, E. B.; Gland, J. L. *Surf. Sci.* **1986**, *172*, 668.

(27) (a) Maca, F.; Scheffler, M.; Berndt, W. *Surf. Sci.* **1985**, *160*, 467. (b) Patterson, C. H.; Lambert, R. M. *Surf. Sci.* **1987**, *187*, 339.

(28) Chan, C.-M.; Weinberg, W. H. *J. Chem. Phys.* **1979**, *71*, 3988.

(29) Wong, P. C.; Zhou, M. Y.; Hui, K. C.; Mitchell, K. A. R. *Surf. Sci.* **1985**, *163*, 172.

(30) Widrig, C. A.; Alves, C. A.; Porter, M. D. *J. Am. Chem. Soc.* **1991**, *113*, 2805.

(31) Prince, N. P.; Seymour, D. L.; Ashwin, M. J.; McConville, C. F.; Wodruff, D. P.; Jones, R. G. *Surf. Sci.* **1990**, *230*, 13.

(32) Ruan, L.; Stensgaard, I.; Besenbacher, F.; Laegsgaard E. *Ultramicroscopy* **1992**, *42$-$44*, 498.

(33) Forbes, J. G.; Gellman, A. J.; Dunphy, J. C.; Salmeron, M. *Surf. Sci.* **1992**, *279*, 68.

(34) Mebrahtu, T; Bothwell, M. E.; Harris, J. E.; Cali, G. J.; Soriaga, M. P. *J. Electroanal. Chem.* **1991**, *300*, 487.

(35) Schwaha, K.; Spencer, N. D.; Lambert, R. M. *Surf. Sci.* **1979**, *81*, 273.

(36) Dhirani, A.; Hines, M. A.; Fisher, A. J.; Ismail, O.; Guyot-Sionnest, P. *Langmuir* **1995**, *11*, 2609.

(37) Cotton, F. A., Wilkinson, G. *Advanced Inorganic Chemistry*, 4th ed.; John Wiley & Sons: New York, 1980; p 505.

(38) Lister, T. E.; Stickney, J. L. *J. Phys. Chem.* **1996**, *100*, 19568.

(39) Foresti, M. L.; Innocenti, M.; Kobayashi, H.; Pezzatini, G., Guidelli, R. *J. Chem. Soc., Faraday Trans.* **1996**, *92*, 3747.

(40) Foresti, M. L.; Aloisi G. D.; Innocenti, M.; Kobayashi, H.; Guidelli, R. *Surf. Sci.* **1995**, *335*, 241.